

POPULATION STUDY OF CANONICAL PULSARS

M. Sautron¹

Abstract. Pulsars are highly magnetized rotating neutron stars, emitting in a broad electromagnetic energy range. These objects have been discovered more than 50 years ago and are astrophysical laboratories for studying physics at extreme conditions. Reproducing the observed population of pulsars refines our understanding of their formation, evolution as well as radiation processes and geometry. The aim of this study is to improve a previous pulsar population synthesis by studying the impact of the Galactic gravitational potential and of the death line putting emphasis on the γ -ray pulsar population. In order to elucidate the necessity of a death line, refined initial distributions for spin periods and radial positions at birth were implemented, elevating the sophistication of these simulations to the most recent state-of-the-art. This pulsar population synthesis takes into account the secular evolution of a force-free magnetosphere and the magnetic field decay. Each pulsar is evolved from its birth up to the present time. The radio and γ -ray emissions are modeled respectively by the polar cap geometry and the striped wind model. This study successfully reproduced the canonical pulsars population with a high degree of similarity, as validated by Kolmogorov-Smirnov (KS) tests on the distributions of P and \dot{P} . Moreover, it is shown that a direct effect of the Galactic potential is to make pulsars lose their alignment between rotation axis and proper motion. Finally, simulations with a higher γ -ray instrumental sensitivity show that the GeV excess in the Galactic centre could be of pulsar origin.

Keywords: pulsars: general, radio continuum: stars, Gamma rays: stars, methods: statistical

1 Introduction

Thanks to radio surveys, performed for instance by the Parkes and Arecibo radio-telescopes, nearly 3000 pulsars have been discovered (Manchester et al. 2005). Although pulsars were first observed in radio, it was found later that they are also bright in X-rays, optical and gamma-rays. The Large Area Telescope (LAT) on board of the Fermi satellite, has discovered dozens of radio-quiet gamma-ray pulsars as well as millisecond pulsars (MSPs). Since its launch, the LAT has detected about 300 pulsars (Abdo et al. 2013; Smith et al. 2019, 2023). With the advent of future surveys such as the Square Kilometre Array (SKA^{*}) or the Cherenkov Telescope Array (CTA[†]), much more pulsars are expected to be detected. Those instruments are scheduled to start collecting data by the end of the decade. SKA is going to be 50 times more sensitive and is predicted to survey the sky 10 000 times faster than any existing imaging radio telescope (McMullin et al. 2020). CTA is aimed at detecting gamma rays in the energy range from a few tens of GeV up to hundreds of TeV (Hofmann & Zanin 2023) while Fermi/LAT operates in the energy range from 20 MeV to several hundred GeV[‡]. Pulsar population synthesis (PPS) is a powerful tool aiming at predicting the discovery rate of new pulsars as well as better understanding their emission processes. PPS studies also constrains the overall properties of pulsars. In these studies, pulsars are generated from their birth and evolved up to the present. Once the set of pulsars has been generated we check whether they fulfill some prescribed detection criteria. The detectability of an individual pulsar in a given energy band (radio or γ) depends on whether the associated emission beam intersects our line of sight and on the sensitivity of the corresponding instrument. This work is an overall improvement of the PPS proposed by Dirson et al. (2022) to reproduce the canonical pulsars population (pulsars which are not magnetars and which are not recycled pulsars) by adding the effect of the Galactic gravitational potential, the interstellar medium (ISM) interaction with the pulsars' radio photons, a death line, more up-to-date distributions at birth and the possibility to have different magnetic field decay timescale for the generated pulsars.

¹ Université de Strasbourg, CNRS, Observatoire astronomique de Strasbourg, UMR 7550, 67000 Strasbourg, France

^{*}<https://www.skao.int/en/science-users/118/ska-telescope-specifications>

[†]<https://www.cta-observatory.org/about/how-ctao-works/>

[‡]<https://fermi.gsfc.nasa.gov/science/instruments/table1-1.html>

2 Generation of pulsars

The value chosen for the birth rate, which is 41 yr^{-1} , is taken as best educated guess from the interval $[33, 150] \text{ yr}^{-1}$ because these studies (Faucher-Giguère & Kaspi 2006; Gullon et al. 2014; Johnston & Karastergiou 2017) evaluated the birth rate of pulsars in this interval. The initial spatial distribution in altitude and the radial spread (in order to have the pulsars born in the spiral arms of the Galaxy, the Galactic spiral structure and the rotation of the Galaxy are also taken into account) used for the pulsars is given by Paczynski (1990) and by Ahlers et al. (2016) (see equations 2.1).

$$\rho_z(z) = \frac{e^{-|z|/h_c}}{h_c}, \rho(R) = A \left(\frac{R + R_1}{R_\odot + R_1} \right)^a \exp \left(-b \left(\frac{R - R_\odot}{R_\odot + R_1} \right) \right) \quad (2.1)$$

where R is the axial distance from the z -axis, and z is the distance from the Galactic disc. The numerical values for the constants are, $A = 37.6 \text{ kpc}^{-2}$, $a = 1.93$, $b = 5.06$, $R_1 = 0.55 \text{ kpc}$, $h_c = 180 \text{ pc}$ and $R_\odot = 8.5 \text{ kpc}$ and in agreement with the distribution of young massive stars in our galaxy (Li et al. 2019). The inclination angle α is assumed to follow an isotropic distribution generated from a uniform distribution $U \in [0, 1]$ and given by $\alpha = \arccos(2U - 1)$. In this work, the initial spin period P_0 and magnetic field B_0 are both following a log-normal distribution (see equation 2.2, where X could be P or B), as suggested from the results of a study of 56 young neutron stars by Igoshev et al. (2022)

$$p(\log(X_0)) = \frac{1}{\sigma_x \sqrt{2\pi}} e^{-(\log X_0 - \log \bar{X})^2 / (2\sigma_x^2)} \quad (2.2)$$

According to Hobbs et al. (2005) a Maxwellian distribution best replicates the observations for the kick velocities at birth, with a standard deviation $\sigma_v = 265 \text{ km/s}$. The mean velocity of the distribution is related to the standard deviation by $\bar{v} = \sigma_v \sqrt{8/\pi} \approx 423 \text{ km/s}$.

3 Evolution

The pulsar force-free magnetosphere model taking into account the plasma current and charge within the magnetosphere is applied. The main equation of this model is equation 3.1

$$\dot{\Omega} = - \frac{4\pi R^6 B^2 (1 + \sin^2 \alpha)}{\mu_0 c^3 I} \Omega^n \quad (3.1)$$

n is the braking index, its value being $n = 3$ for magnetic dipole radiation, $\Omega = 2\pi/P$ is the rotation frequency of the pulsar (P is the spin period) and $\dot{\Omega}$ is its time derivative. I is the moment inertia of the neutron star, its value being approximately $I \approx 10^{38} \text{ kg.m}^2$, $R = 12 \text{ km}$ is the typical radius of a neutron star, μ_0 is the vacuum permeability constant, $\mu_0 = 4\pi \times 10^{-7} \text{ H/m}$ and c is the speed of light. A magnetic field decay is prescribed according to a power law

$$B(t) = B_0 (1 + t/\tau_d)^{-1/\alpha_d} \quad (3.2)$$

where $\alpha_d = 1.5$ is a constant parameter controlling the speed of the magnetic field decay and $\tau_d = k_{\tau_d} \tau_v$ is the magnetic field decay time scale. The decay rate τ_v was chosen randomly between 3 values : $5 \times 10^4 \text{ yr}$ or $7 \times 10^4 \text{ yr}$ or $5 \times 10^5 \text{ yr}$, with a probability of 0.23, 0.46 and 0.31 respectively (these probabilities were chosen as best educated guesses after several run with different values) for each pulsar, corresponding to the τ_v value for canonical pulsars in Viganò et al. (2013) and $k_{\tau_d} = 5$.

Finally, we need to follow the particle motion within the Galactic potential. Each generated pulsar evolves in the gravitational potential Φ subject to an acceleration $\ddot{\mathbf{x}}$ according to

$$\ddot{\mathbf{x}} = -\nabla\Phi. \quad (3.3)$$

4 Detection

In a nutshell, in radio a pulsar is going to be considered as detected if its signal to noise ratio is greater or equal to 10 (in this signal to noise ratio, the flux in radio, the observed pulse profile which takes into account the interaction of the ISM and the parameters of the Parkes Multibeam Pulsar Survey (PMPS) are taken into account) and it will be considered detected in γ -ray if its flux in this wavelength band is greater than

the expectation of the Fermi/LAT instrument [§]. It is also needed to see a pulsation (in radio or γ -ray) from Earth, which depends on the geometry of emission and the position of the pulsar in the simulation. Finally, the detection will not count if a simulated pulsar crossed the death line proposed by Mitra et al. (2019), in this work it is even a death valley, since it is considered that the parameters of the death line can vary from one pulsar to another, making the death line appear at a different position from each pulsar.

5 Results

The left panel of Fig. 1 allows to observe both the population of canonical pulsars of the observations (in blue) and the results of the simulation (in red) in the $P - \dot{P}$ diagram when 1 million pulsars are simulated. A KS test was conducted for both distributions P and \dot{P} and yielded p-values of 0.24 and 0.07 respectively, which means the null hypothesis that observations and simulations originate from the same distribution for the spin period can not be rejected at a 5 percent confidence level (p-value ≥ 0.05). Moreover, no pile up effect is observed next to the death line, while it often happens in other studies.

Concerning the right panel of Fig. 1, it is shown that the old pulsars with an age larger than 10 Myr have a tendency to lose their alignment between rotation axis and velocity, a direct effect of the Galactic potential as shown by the observations of Noutsos et al. (2013), but it is the first time it is done in a simulation.

When we focus on the γ -ray band of the canonical pulsar population we can check the left panel of Fig. 2,

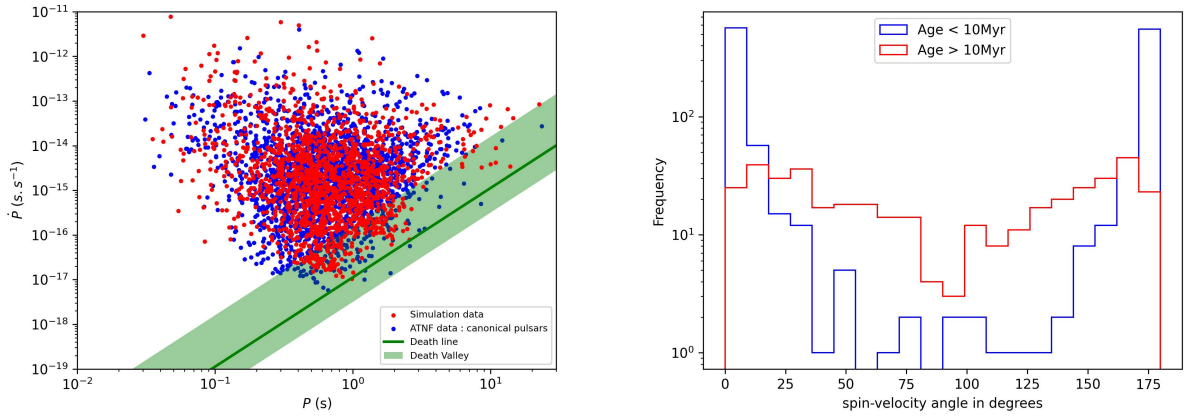


Fig. 1. Left: $P - \dot{P}$ diagram of a simulated population, along with the observations. **Right:** Distribution of the spin-velocity angles for the detected pulsars younger than 10 Myr (blue) and pulsars older than 10 Myr (red) in the simulation.

where we have a $P - \dot{P}$ diagram of this part of the population. The simulated gamma-ray pulsars are in the same area of the plot as the observed pulsars, meaning the striped wind model allow to correctly reproduce these pulsars. Nevertheless, the total number of pulsars detected in gamma-ray is significantly larger in our simulation compared to the observations (154 simulated and 63 observed), when using the Fermi/LAT instrument sensitivity, which means many sources unidentified in the Fourth Fermi-LAT Catalog of Gamma-ray sources (4FGL) could be pulsars.

The right panel of Fig. 2 is the position of the detected pulsars in γ -ray in the Galactic plane, when a simulation was run with an increased sensitivity of a factor 10 compared to the sensitivity of the Fermi/LAT instrument. The red dots correspond to the pulsars which would have been detected with the sensitivity of the Fermi/LAT instrument, and the green dots correspond to the pulsars detected thanks to the increased sensitivity (as can be seen in the caption of Fig. 2, there are two different thresholds for the minimum detectable flux, depending on if we consider it a blind search or not. In that case for the Fermi/LAT instrument the threshold is $F_{min} = 16 \times 10^{-15} \text{ W.m}^{-2}$, otherwise it is $F_{min} = 4 \times 10^{-15} \text{ W.m}^{-2}$). We detect 11 times more γ -ray pulsars, obviously we detect more pulsars close to us, and also many more in the centre of the Galaxy. This result

[§]https://fermi.gsfc.nasa.gov/ssc/data/analysis/documentation/Cicerone/Cicerone_LAT_IRFs/LAT_sensitivity.html

indicates that the GeV excess in the Galactic centre could be linked to pulsars not yet identified, while usually the hypothesis is that the GeV excess corresponds to self-annihilating dark matter particles (Hooper 2022).

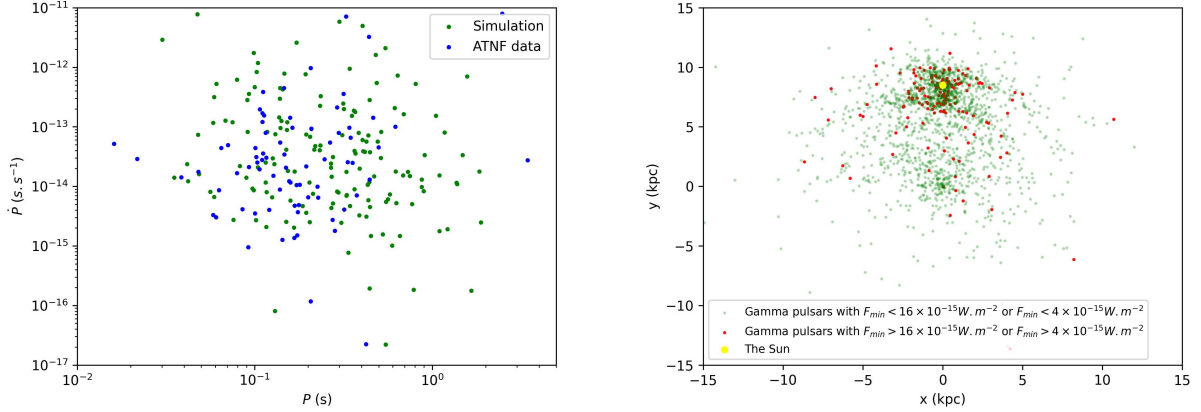


Fig. 2. **Left:** $P - \dot{P}$ diagram of the gamma-only pulsars for both the simulations and the observations. **Right:** Spatial distribution of the simulated gamma-ray detected pulsars, projected onto the Galactic plane.

6 Conclusions

In summary, the best parameters found for this pulsar population synthesis are for $\bar{P} = 129$ ms, $\sigma_p = 0.45$ for the spin period distribution at birth, $\bar{B} = 2.75 \times 10^8$ T, $\sigma_b = 0.5$ for the magnetic field distribution at birth and for a birth rate of 41 yr^{-1} . Ultimately, this work provides a simulated population of pulsars within the Milky Way more similar to the observations compared to Dirson et al. (2022). Moreover, such investigations will be useful to make more predictions for future radio or γ -ray surveys such as SKA, NenuFAR or CTA. The PPS method used in this study is going to be applied in a near future to model populations of pulsars in the Milky Way other than the canonical ones, the magnetars and the millisecond pulsars.

References

- Abdo, A., Ajello, M., Allafort, A., et al. 2013, ApJS, 208
 Ahlers, M., Bai, Y., Barger, V., et al. 2016, Physical Review D, 93
 Dirson, L., Pétri, J., & Mitra, D. 2022, A&A, 667
 Faucher-Giguère, C.-A. & Kaspi, V. 2006, ApJ, 643
 Gullon, M., Miralles, J., Viganò, D., et al. 2014, MNRAS, 443
 Hobbs, G., Lorimer, D., Lyne, A., et al. 2005, MNRAS, 360
 Hofmann, W. & Zanin, R. 2023, eprint arXiv:2305.12888
 Hooper, D. 2022, 14th International Conference on Identification of Dark Matter, Vienna, Austria, eprint arXiv:2209.14370
 Igoshev, A., Frantsuzova, A., Gourgouliatos, K., et al. 2022, MNRAS, 514
 Johnston, S. & Karastergiou, A. 2017, MNRAS, 467
 Li, C., Zhao, G., Jia, Y., et al. 2019, ApJ, 871
 Manchester, R., Hobbs, G., Teoh, A., et al. 2005, AJ, 129, 1993
 McMullin, J., Diamond, P., McPherson, A., et al. 2020, Proceedings of the SPIE, 11445
 Mitra, D., Basu, R., Melikidze, G., et al. 2019, MNRAS, 492
 Noutsos, A., Schnitzeler, D., Keane, E., et al. 2013, MNRAS, 430
 Paczynski, B. 1990, ApJ, 348
 Smith, D., Abdollahi, S., Ajello, M., et al. 2023, ApJ, 958
 Smith, D., Bruel, P., Cognard, I., et al. 2019, ApJ, 871
 Viganò, D., Rea, N., Pons, J., et al. 2013, MNRAS, 434